

1 Supporting Information

2 **Impact of Pt Particle Size Distribution on HER Pathway and Performance**

3

4 Yintong Zhou ^{a, #}, Dayu Xiang^{a, #}, Jiayao Mao^a, Hanling Tie^a, Rongsheng Chen^{a,*},

5 Jiaxing Wang^a, Feng Ma^a, Huimin Wang^b, Xiaohui Ren^{b,*}, Hongwei Ni^b

6 ^a Institute of Steel and Chemicals Co-Production, School of Chemistry and Chemical

7 Engineering, Wuhan University of Science and Technology, Wuhan 430081, China

8 ^b Key Laboratory for Ferrous Metallurgy and Resources Utilization of Ministry of

9 Education & Hubei Provincial Key Laboratory for New Processes of Ironmaking and

10 Steel making, School of Metallurgy and Energy, Wuhan University of Science and

11 Technology, Wuhan, 430081 China, Wuhan University of Science and Technology,

12 Wuhan 430081, China

13 **Corresponding authors:** Dr. Prof. Xiaohui Ren (Email: xhren@wust.edu.cn); Dr.

14 Prof. Rongsheng Chen (chenrs@wust.edu.cn)

15

1 **1. Experimental**

2 **1.1 Materials**

3 All chemicals were purchased from reagent companies and used directly without
4 further purification. Dopamine ($C_8H_{11}NO_2$, 98%) was purchased from Shanghai
5 Aladdin Biochemical Technology Co., Ltd. Tris hydrochloride ($C_4H_{11}NO_3$, 99.9%) was
6 obtained from Saiguo Biotechnology Co., Ltd. Pluronic P123 ($EO_{20}PO_{70}EO_{20}$, BR) was
7 purchased from Energy Chemical. Trimethylbenzene (C_9H_{12} , 99.7%), ethanol
8 (C_2H_5OH , 99.7%), and sulfuric acid (H_2SO_4 , 99.7%) were all purchased from
9 Sinopharm Chemical Reagent Co., Ltd. Chloroplatinic acid (H_2PtCl_6 , 99.9%) was
10 acquired from Shanghai Macklin Biochemical Technology Co., Ltd. The 20%
11 commercial Pt/C (20%-Pt/C, 20%) was purchased from JM Company (USA). Nafion
12 perfluorosulfonic acid resin ($C_7HF_{13}O_5SC_2F_4$, 10%) was obtained from Shengernuo
13 Technology Co., Ltd.

14 **1.2 Synthesis of PDA Nanospheres**

15 2 g of 3,3',5,5'-tetramethylbenzidine (TMB) and 2 g of Pluronic F-127 (F127) were
16 added to the aqueous phase (250 mL of water + 250 mL of trimethylbenzene)
17 respectively. After being stirred uniformly, the mixture was sonicated for 30 minutes.
18 Then, an appropriate amount of tris(hydroxymethyl)aminomethane (approximately 100
19 mg) was added to adjust the pH of the solution to 8.5. Subsequently, 600 mg of DA was
20 added, and the mixture was stirred at room temperature for 24 hours. The product was
21 washed twice with alcohol and ethanol respectively, centrifuged, and then placed in a
22 blast drying oven for 24 hours to obtain PDA nanospheres. The size of PDA
23 nanospheres was regulated by changing the polymerization time (8 h, 16 h, 24 h, and
24 32 h respectively), resulting in PDA nanospheres with sizes of 130 nm, 200 nm, 400
25 nm, and 550 nm.

26 **1.3 Synthesis of Pt/C Catalysts**

27 100 mg of PDA nanospheres were weighed and dissolved in distilled water. After

1 ultrasonic homogenization, 26.34 mg of H_2PtCl_6 was added, and the mixture was stirred
2 at room temperature for 24 hours. Then, it was washed twice with alcohol and distilled
3 water respectively, centrifuged, and placed in a blast drying oven for 24 hours to obtain
4 Pt/C catalyst precursors with Pt^{4+} supported on PDA nanoparticles of different sizes.
5 Subsequently, the samples were placed in a tube furnace and subjected to carbonization
6 treatment at 1000 °C under the protection of N_2 inert atmosphere, yielding Pt/C-130,
7 Pt/C-200, Pt/C-400, and Pt/C-550 catalysts. The carbonization temperature of 1000 °C
8 was determined as the optimal annealing temperature for the Pt/C-200 catalyst after
9 annealing at different temperatures.

10 **1.4 Physical characterization**

11 The morphology of the catalyst samples was characterized using a scanning
12 electron microscope (SEM, TESCAN VEGA, Czech Republic). The composition of the
13 catalysts was analyzed by X-ray diffraction (XRD, Rigaku SmartLab SE, Japan).
14 Additionally, the microstructure and crystallographic information of the catalysts were
15 characterized via transmission electron microscopy (TEM, FEI Tecnai G2 F20, Japan).
16 The surface elemental species and chemical bonds of the catalysts were determined
17 using X-ray photoelectron spectroscopy (XPS, Thermo Scientific K-Alpha+, USA).
18 The elemental contents in the catalysts were measured by inductively coupled plasma
19 mass spectrometry (ICP-MS, Agilent 720, USA).

20 **1.5 Electrochemical characterization**

21 All the HER electrochemical performance tests in this experiment were conducted
22 using a three-electrode system on a Chenhua CHI660E electrochemical workstation. A
23 0.5 M H_2SO_4 solution was used as the electrolyte, with an Ag/AgCl electrode as the
24 reference electrode, a graphite rod as the counter electrode, and a glassy carbon
25 electrode (with a diameter of 3 mm) drop-coated with the catalyst as the working
26 electrode. Specifically, 2 mg of the catalyst was weighed and added, along with 20 μL
27 of Nafion, to a mixed solution composed of 600 μL of water and 400 μL of isopropanol.
28 Subsequently, this mixture was subjected to ultrasonic treatment for 30 minutes to

1 obtain a uniformly dispersed liquid. Using a pipette, 5 μL of this dispersion was dropped
2 onto the surface of the glassy carbon electrode. The catalyst suspension was dried under
3 infrared lamp illumination to prepare the working electrode for subsequent
4 electrochemical tests.

5 **Linear Sweep Voltammetry (LSV) Tests:** The LSV tests were performed at a scan
6 rate of 5 mV s^{-1} within the voltage range of -0.2 V to -0.7 V . All test results were
7 corrected with 90% iR compensation according to the equation: $E_{\text{correct}} = E_{\text{RHE}} - iR_s$,
8 where R_s represents the solution resistance obtained from EIS. The Tafel curves were
9 derived by processing the LSV test data according to Equation (1), and the reaction
10 pathway in the HER process was determined based on the Tafel slope:

$$11 \quad \eta = a + b \lg |j| \quad (1)$$

12 where b is the Tafel slope and j is the current density.

13 **Electrochemical Impedance Spectroscopy (EIS) Tests:** The EIS tests on the
14 catalysts were carried out over a frequency range of 10^{-2} to 10^5 Hz with an amplitude
15 of 5 mV .

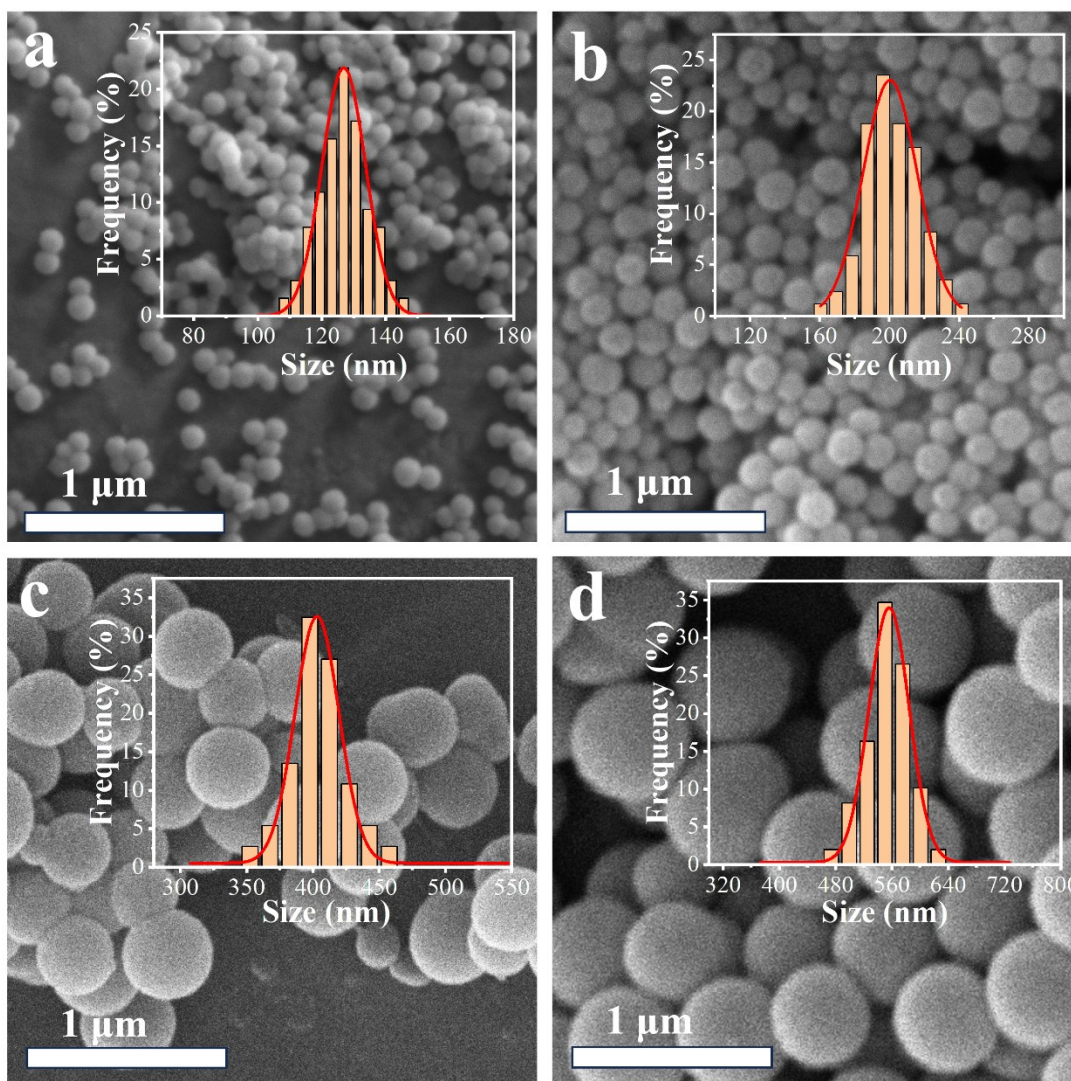
16 **Measurement of Electrochemical Active Surface Area via Hydrogen Adsorption-**
17 **Desorption Method:** Cyclic voltammetry scans were performed within an appropriate
18 potential range. During the scanning process, the curve of current versus potential was
19 recorded. When the potential was scanned from negative to positive, the hydrogen
20 atoms adsorbed on the catalyst surface underwent desorption, resulting in an obvious
21 desorption current peak. The obtained curve was integrated to calculate the charge of
22 the hydrogen desorption peak (QH). The electrochemical active surface area of the
23 catalyst was calculated using Equation (2) based on the known charge for hydrogen
24 adsorption per active site (theoretical value $Q_0 = 210 \mu\text{C}/\text{cm}^2$):

$$25 \quad \text{ECSA} = \frac{QH}{Q_0 * m} \quad (2)$$

26 where m is the mass of the catalyst.

27

1

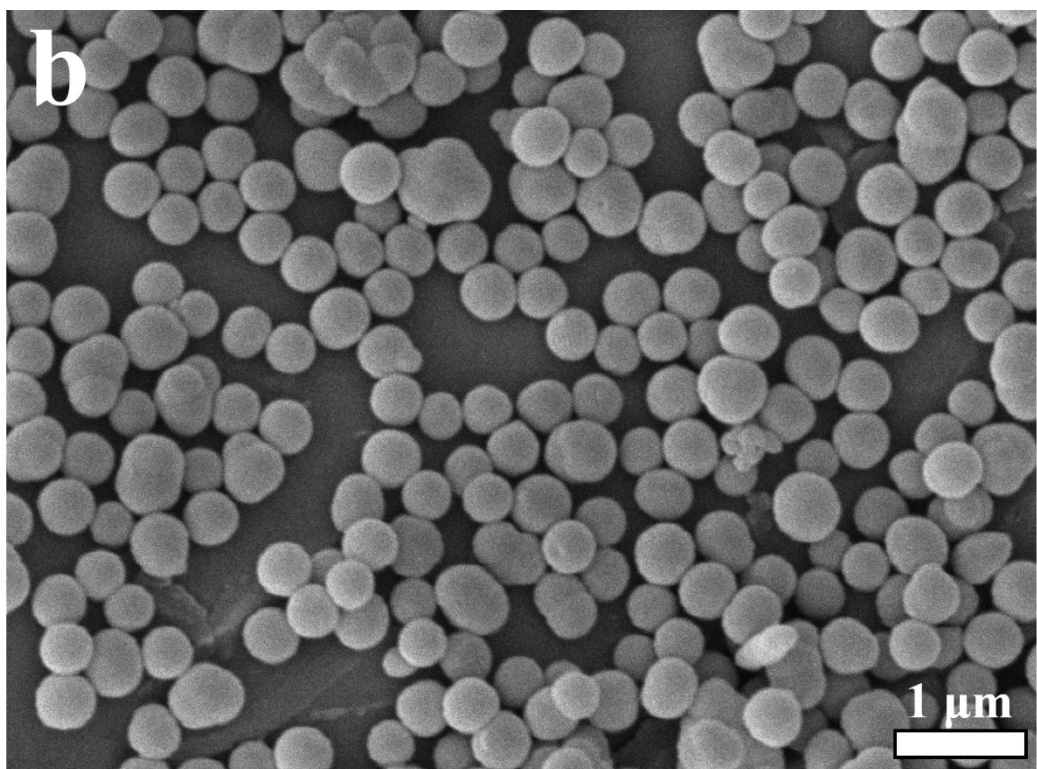
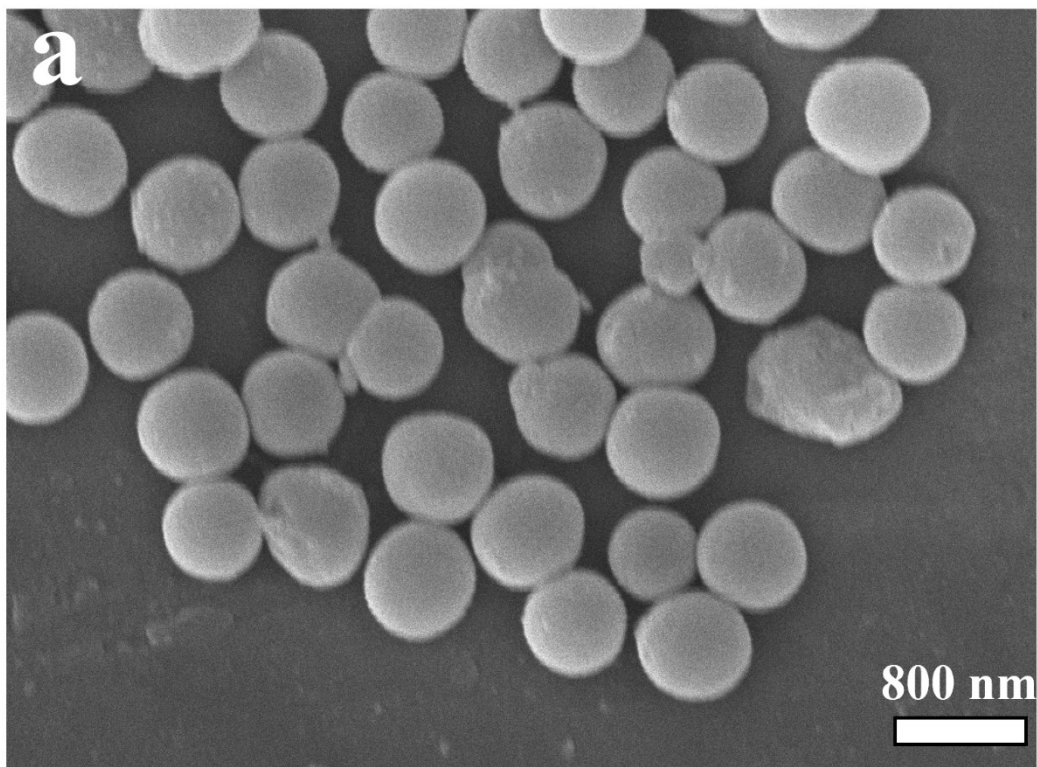


2

3 **Fig. S1.** Morphology and Size of Pt⁴⁺-Loaded PDA Nanospheres with Different Sizes: (a) 130 nm;

4 (b) 200 nm; (c) 400 nm; (d) 550 nm

1

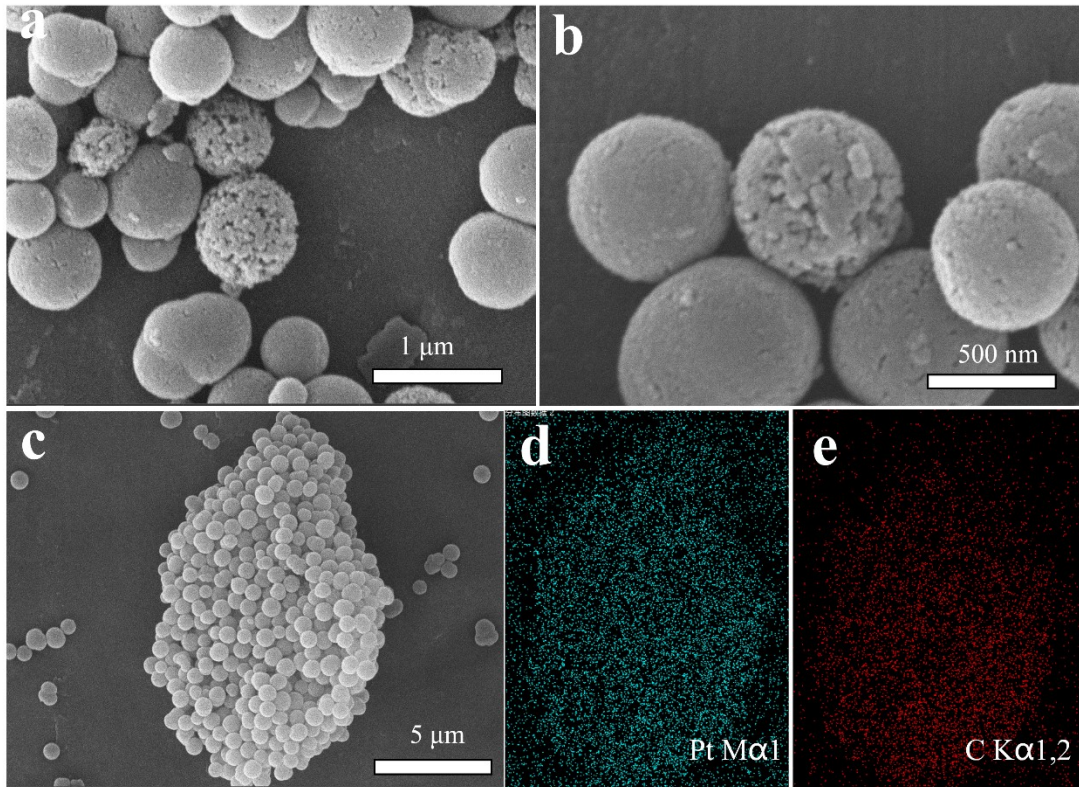


2

3 **Fig. S2.** SEM Morphologies of Pt/CS-200 Before and After Carbonization: (a) Before

4 Carbonization; (b) After Carbonization

1

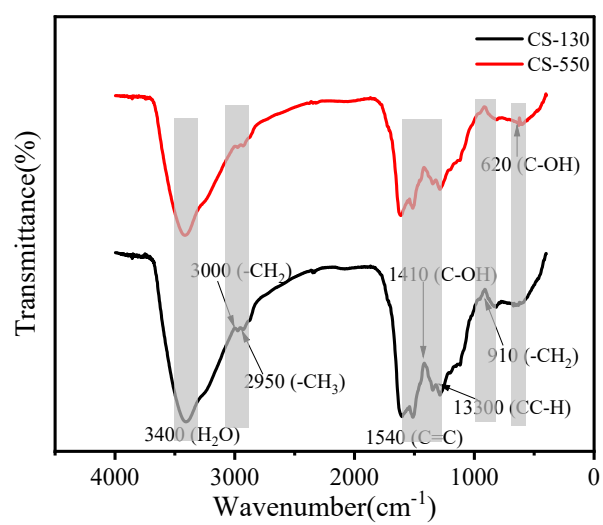


2

3 **Fig. S3.** Morphological and Elemental Composition Analysis of Pt/CS-550: (a-c) SEM

4 Morphology Images; (d, e) EDS Mapping Results

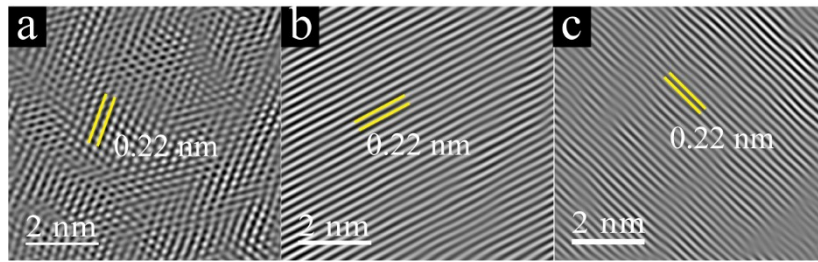
5



1

2 **Fig. S4.** Comparison of FTIR spectra for PDA carbon spheres with CS-130 and CS-550.

1



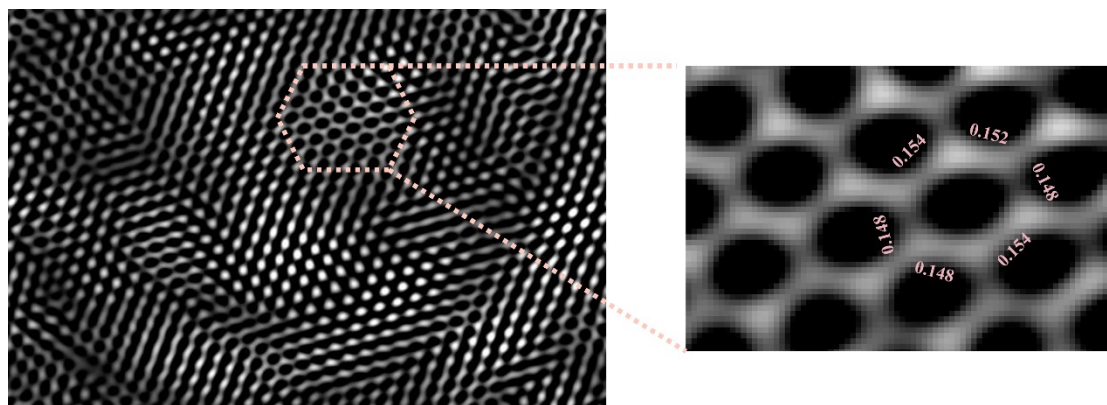
2

3 **Fig. S5.** (a–c) Inverse FFT images (IFFT) corresponding to regions 1#, 2#, and 3# in Fig. 2(g),

4 respectively.

5

1

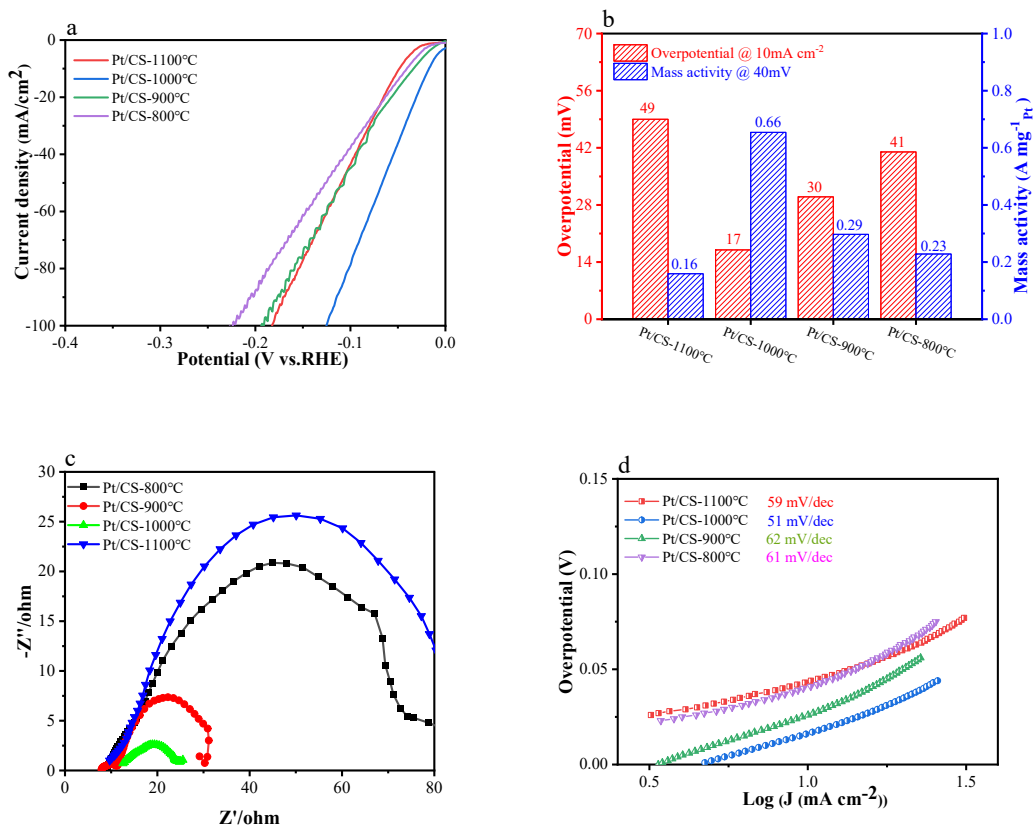


2

3 **Fig. S6.** Surface Structural Analysis of Pt/CS-200

4

5



1

2

3

4 **Fig. S7.** Pt/CS-200 at different carbonization temperatures: (a) LSV curves; (b)

5 Overpotential at 10 mA cm⁻² and mass activity at 40 mV (bar chart); (c)

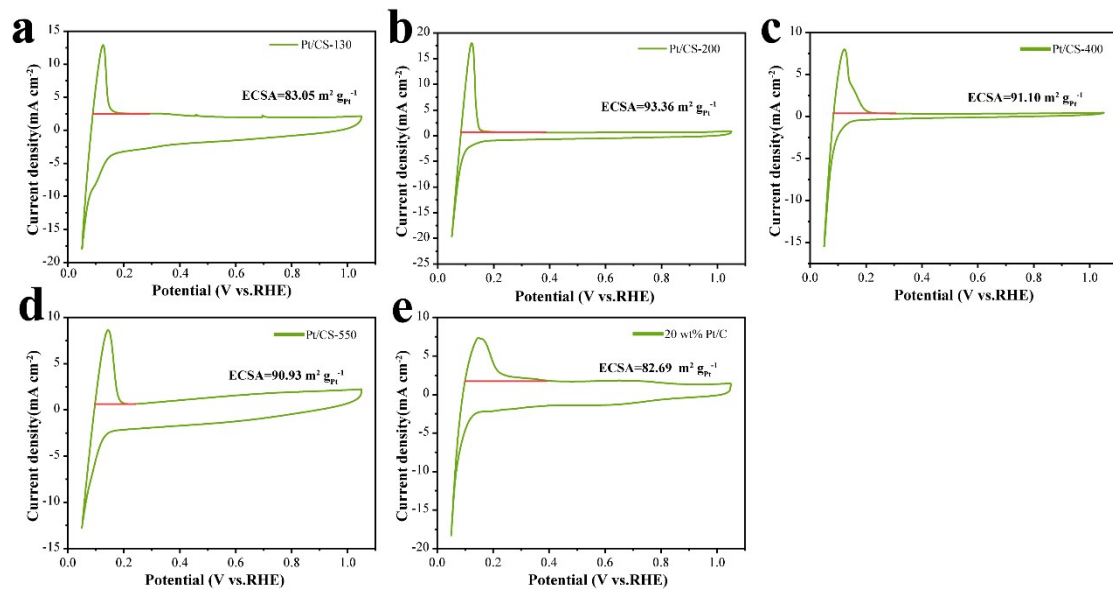
6 Electrochemical impedance spectra; (d) Tafel slopes.

7

8

9

1



3

4 **Fig. S8.** Hydrogen Adsorption Test: Electrochemical Active Surface Area (ECSA) of

5 Pt/CS-130 (a), Pt/CS-200 (b), Pt/CS-400 (c), Pt/CS-550 (d), and Commercial 20%-Pt/C

6 (e).

7

1 Table S1. The fitting impedance parameters of Pt/CS-130, Pt/CS-200, Pt/CS-400,
2 Pt/CS-550, and 20% wt Pt/C.

	Rs	Rct	CPE-T	CPE-P
Pt/CS-130	10.5	15.4	0.00122	0.500
Pt/CS-200	12.2	13.4	0.000679	0.530
Pt/CS-400	9.8	15.8	0.00106	0.663
Pt/CS-550	12.3	29.6	0.00103	0.706
20% wt Pt/C	8.7	17.2	0.000188	0.691

3

4 Table S2. ICP-MS statistics of Pt content of Pt/CS-130, Pt/CS-200, Pt/CS-400, and

5 Pt/CS-550

samples	Pt content (wt%)
Pt/CS-130	12.37
Pt/CS-200	15.05
Pt/CS-400	15.98
Pt/CS-550	11.77

6

7 Table S3. Comparison of synthetic approach and HER activity of reported
8 electrocatalysts under 0.5 M H₂SO₄ solution.

No.	Catalysts	Overpotential(mV)	Tafel slope (mV/dec)	Ref.
01	Pt/CS-200	17	29.8	This work
02	1 wt% Pt/ Mo ₂ C/C	19	28	[1]
03	g-C ₃ N ₄ @Pt	100	77	[2]
04	Pt NPs/DPC	30	31	[3]
05	L-PtNi-C	38	29.6	[4]
06	Pt/CoNC	15.2	45.6	[5]
07	C-ZIF-CuPt	46	45	[6]
08	Pt/C-0.2	17	48.43	[7]
09	Pt ₁ %-CoMoS ₂ /C	118	68	[8]
10	Pt-WC-1,10/BMZ	23	40.1	[9]
11	Pt NCs	42	101	[10]
12	L-Pt/SC	23	24	[11]
13	C-rPDA-Pt/TiO ₂ NSs	60	34.8	[12]

1

2 Refences

3

- 4 1. T. Ping, S. V. Purohit, S. P. Sahu, B. Dash and B. K. Jena, *Langmuir*, 2025, **41**,
- 5 3392-3401.
- 6 2. A. Sharma, H. Devnani, J. P. Singh, M. Varshney and H. J. Shin, *Current*
- 7 *Applied Physics*, 2025, **77**, 39-45.
- 8 3. X. Liu, K. Wang, Y. Li, Y. Wang, B. Liu, P. Zhang and B. Xu, *Journal of Alloys*
- 9 *and Compounds*, 2023, **968**, 171970.
- 10 4. Y. Fu, X. Xu, R. Lin, Y. Yang, Y. Wu, N. Li, H. Wang, Q. Li and J. Qian,
- 11 *Inorganic Chemistry*, 2025, **64**, 16615-16622.
- 12 5. Q. Zheng, W. An, J. X. Pan, F. S. Yu, Y. Z. Du, J. Cui, W. Y. Song, S. M. Xu, C.
- 13 X. Wang, G. Y. Huang and Y. M. Yan, *Susmat*, 2025, **5**, e266.
- 14 6. C. Wang, L. Kuai, W. Cao, H. Singh, A. Zakharov, Y. Niu, H. Sun and B. Geng,
- 15 *Chem Eng J*, 2021, **426**, 130749.
- 16 7. X. Zhou, J. Zhang, X. Lan, Z. Jiao, B. Liu, Y. Wang, P. Zhang and B. Xu,
- 17 *Journal of Alloys and Compounds*, 2024, **1005**, 176195.
- 18 8. L. A. Zavala, K. Kumar, V. Martin, F. Maillard, F. Maugé, X. Portier, L.
- 19 Oliviero and L. Dubau, *ACS Catalysis*, 2023, **13**, 1221-1229.

- 1 9. X. Chen, S. Li, X. Sun, F. Liu, C. Li, J. Yu and S. Mu, *Electrochim Acta*, 2019,
2 **328**, 135077.
- 3 10. H. Tian, X. Cui, L. Zeng, L. Su, Y. Song and J. Shi, *J Mater Chem A*, 2019, **7**,
4 6285-6293.
- 5 11. Y. Wen, J. X. Wang, D. Li, Y. T. Chen, X. H. Ren, F. Ma, X. T. Liu, G. J. Cheng,
6 W. Z. Cao, W. P. He, X. X. Jiang, T. Zhang, R. S. Chen and H. W. Ni, *Small*
7 *Methods*, 2024, **9**, 2401095.
- 8 12. J. Y. Mao, J. Y. Zhao, J. X. Wang, Y. Chen, Y. Lu, X. Ren, X. Liu, F. Ma, R.
9 Chen and H. Ni, *J Colloid Interf Sci*, 2026, **703**, 139185.
- 10
- 11
- 12